

EPAC BEAMLINE PROTOTYPE: DEVELOPMENT AND OPTIMISATION OF A HIGH-REPETITION-RATE LWFA SYSTEM

K. Fedorov^{†,1}, O. Finlay¹, D. Symes¹, A. Bennett¹, J. Giles-Friend¹, A. Bhardwaj¹, N. Bourgeois¹, C. D. Armstrong¹, C. Selig¹, A. Thomas¹, C. Spindloe¹, R. Pattathil¹, B. Morkot¹, S. J. D. Dann¹, B. Spiers¹, C. Hernandez-Gomez¹, E. Kiely², D. McCartney³, M. Streeter³

¹Central Laser Facility, STFC Rutherford Appleton Laboratory, Didcot, UK

²Warwick Manufacturing Group, University of Warwick, Warwick, UK

³Centre for Light-Matter Interactions, Queen's University Belfast, Belfast, UK

Abstract

The Extreme Photonics Applications Centre (EPAC) is a next-generation high-power laser facility designed to deliver stable, high-repetition-rate (10 Hz) electron beamline with high quality parameters (~ 1 nC, ~ 1 GeV, $< 5\%$ energy spread) produced by laser-wakefield acceleration (LWFA). These beams will serve as drivers for compact secondary sources, including high-brilliance betatron and inverse-Compton X-rays, enabling a broad range of scientific and industrial applications. To de-risk the commissioning of EPAC, Target Area 2 (TA2) of the Central Laser Facility (CLF) Gemini laser has been set up as a prototype beamline, allowing development of reliable gas-cell targetry, identifying beam-instability sources, testing of optimisation routines, and electron transport configurations. Results from the new beamline highlight the feasibility and challenges of achieving multi-hour operation, providing a practical route toward reliable EPAC operation.

INTRODUCTION

Delivering consistent operation of a LWFA beamline in the Extreme Photonics Applications Centre (EPAC) [1] requires stable laser [2] and target behaviour [3] over many hours. Even small variations in plasma density, laser pointing, or optical aberrations can strongly influence beam charge, energy and stability, making it essential to combine durable hardware solutions with advanced optimisation methods. In this work we use the Gemini TA2 prototype beamline as a development platform to investigate gas-cell design and aperture survivability, assess the origins of electron beam fluctuations, and implement Bayesian optimisation routines capable of efficiently tuning multi-parameter control spaces. The TA2 laser system can provide 5 Hz, 400 mJ, 40 fs laser pulses focused to a $20\ \mu\text{m}$ spot (Fig. 1). The laser pulse interacts with the 2-3 mm gas-cell target filled with 98 % He with 2 % N_2 .

TARGETRY DEVELOPMENT

To control the plasma density and profile we have designed a custom gas-cell, maintaining the flexibility of the design in Ref. [4]. The aim was to ensure easy maintenance of the cell, since laser jitter can cause significant damage to the entrance/exit apertures of the cell and blackening of the probe beam windows from debris, especially operating

at 5 Hz repetition rate. The main components of the new design are highlighted in Fig. 2.

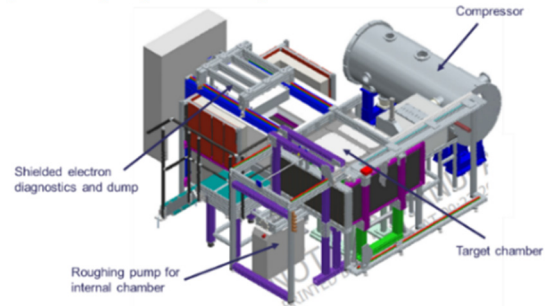


Figure 1: Compact LWFA system in Gemini Target Area 2.

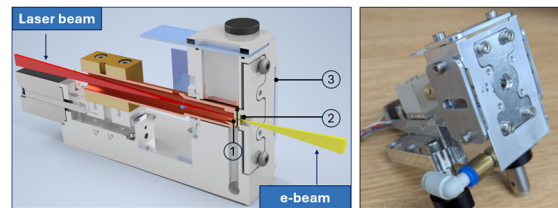


Figure 2: Left: Gas-cell assembly design: 1: replaceable entrance aperture (variable position); 2: replaceable exit aperture; 3: probe beam windows. Right: Assembly with motorised stage to control gas-cell length.

The investigation of both aperture disk thickness and aperture hole diameter, and their influence on the gas density profile, is important for optimising LWFA performance. The aperture hole diameter (e.g., $200\ \mu\text{m}$ entrance, $400\ \mu\text{m}$ exit) determines gas leakage rate, shaping the density across the cell and influencing gas load in the target chamber. At the same time, aperture thickness determines the density ramp length impacting electron injection efficiency and beam stability. A well-optimized combination of these parameters reduces electron energy spread and improves charge [5]. We performed a set of simulations in OpenFOAM software [6] to demonstrate how thicker apertures (up to 1 mm) produce a longer density profile slope, potentially smoothing injection but reducing efficiency, whereas a thinner (down to $300\ \mu\text{m}$) apertures maintain a sharper gradient (Fig. 3 Left). At the same time, increasing entrance/exit hole sizes decrease overall density due to increased leakage (Fig. 3 Right). The dependence of the gas density profile on gas cell configuration, particularly aperture diameters, highlights the importance of studying aperture durability, as they are critically exposed to high-power

[†] Kirill.fedorov@stfc.ac.uk

laser interaction due to shot-to-shot spatial jitter and inhomogeneities of the focused beam profile.

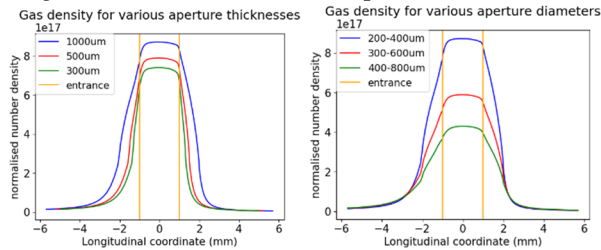


Figure 3: Left: Longitudinal gas density profile for various aperture thickness (400 / 800 μm entrance / exit configuration). Right: Density profile for various entrance / exit configuration (300 μm aperture thickness). Both presented for gas pressure $P = 400$ mbar.

We tested several candidate materials: tungsten, Macor, Sapphire, and CVD diamond. Initially all apertures were made with aperture diameters of 200 μm for entrance and 400 μm for exit to maximise gas density inside the gas cell. Figure 4 demonstrates a comparison of the aperture size before (red circle) and after a number of shots. Number of shots at each candidate material were influenced by electron quality – after significant degradation both apertures were replaced. This approach was subjective and partly coupled with other experimental conditions, thus presented results can be used to discuss damage morphology and only make preliminary conclusions on the choice of material.

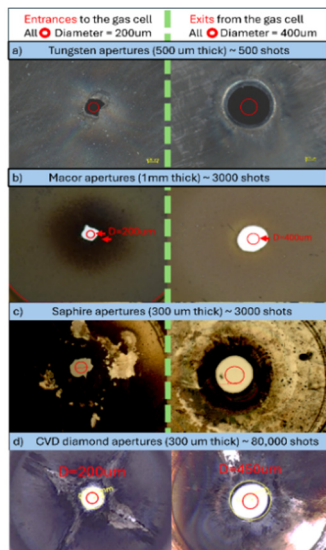


Figure 4: Comparison of the entrance (Left) and exit (Right) aperture size before (red circle) and after number of shots taken.

Unlike tungsten, Macor and sapphire, CVD diamond aperture allowed us to run LWFA setup for more than 80,000 shots. Electron energy spectrum during first 1,000 shots compared with the one during last 1,000 shots in Fig. 5. The difference between damage mechanisms can be seen by comparing different aperture entrances (Fig. 4 Left), where material has been exposed to laser intensities of $\sim 10^{18}$ W/cm² because of pointing jitter. Macor, tungsten and sapphire entrance apertures appear to fracture in

unpredicted asymmetrical ways, whereas CVD diamond is damaged gradually in a circular pattern. To the best of our knowledge damage morphology could influence the quality of the electron beam due to an inhomogeneous density profile when using fractured apertures. The higher damage threshold of CVD diamond can be attributed to extremely high thermal conductivity and hardness [7]. At the same time exit apertures (Fig. 4 Right) are damaged gradually for all candidates, which could be attributed to consistent material removal due to ablation [8]. These findings demonstrate that diamond is a promising material for sustained LWFA operation. Overall, the combination of a gas-cell design with a variable cell length, aperture geometry and robust materials provides a practical pathway toward the reliable targets required for EPAC.

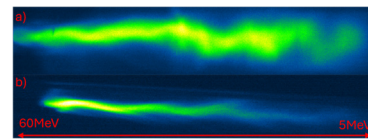


Figure 5: Example of two electron spectra taken during (a) first and (b) last 1,000 shots for diamond apertures.

E-BEAM CHARACTERISATION

To achieve stable, high-performance operation of LWFA beamlines at high repetition rates, we are working on implementation of Bayesian optimisation and laser stabilisation routines. For these methods to be effective, it is essential to identify which input parameters most strongly influence key electron beam characteristics such as charge, energy, divergence, and stability. Figure 6 (a) shows the correlation matrix between typical laser system parameters (in our control) versus electron beam charge. To simplify visualisation, only correlations for pointing in Y, and astigmatism at 0 degree are shown. The energy instability of $\pm 6\%$ causes a $\pm 50\%$ swing in measured electron charge.

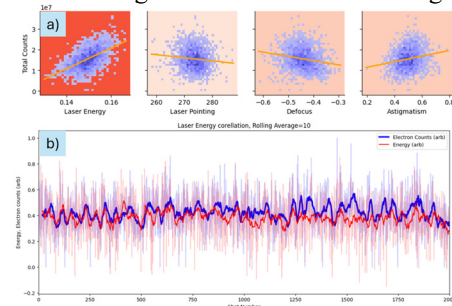


Figure 6: (a) Typical correlation plot; (b) Detailed view of correlation between laser energy and electron charge.

Table 1 summarizes the relative contributions to the stability of electron charge from laser energy and pointing shot-to-shot jitter and long-term drift. Shot-to-shot stability was quantified by subtracting a 20-shot rolling mean from the raw signal to remove slow drifts. The residual jitter was then expressed as a percentage of the overall mean. Under such conditions, predictive stabilisation methods, for example, Gaussian Process Regression models trained on correlated parameters, may be used to suppress mid-term and long-term instabilities.

Table 1: Contributions to the Stability of Electron Charge from Laser Energy and Pointing Instabilities

Parameter	Over-all variation	Fast jitter	Slow drift	Charge correlation (arb.)
Laser energy (J)	3.6	2.5	1	0.56
Laser pointing (μ rad)	6.3	2.5	3.7	-0.12
Resulting impact: Charge (%counts)	32	18	13	

BAYESIAN OPTIMIZATION OF E-BEAM

For EPAC, we will need to optimise a multi-dimensional parameter space to achieve the required radiation conditions for given experimental requirements. In practice, this means selecting and tuning machine Control Inputs to produce specific laser–plasma interaction conditions, which in turn determine the resulting electron and secondary photon beams. The relationships between controls, underlying physics, and outputs are often non-linear, coupled, and may involve parameters that cannot be adjusted or measured.

Table 2: Linked Layers of LWFA Optimisation Concept

Layer	Description	Examples
Control Inputs	Parameters that can be directly adjusted on the machine and indirectly set the physics conditions.	Laser timing, dazzler settings, pointing, AO settings, gas pressure, gas length.
Physics Inputs	Physical parameters determined by the control inputs. Require diagnostics to verify.	Laser energy, pulse duration, focal quality and position, gas density / profile
Physics Outputs	Physical parameters describing output electrons/X-rays.	Electrons / X-rays flux, divergence energy, energy spread, etc
Measured Outputs	Detector-level signals. Direct feedback channels for optimisation.	E-spec images, beam profiles, x-ray camera images

To efficiently explore and use this complex space, we will employ Bayesian optimisation. This method combines an internal predictive model of the experiment with an acquisition function that balances exploration (testing new parameter regions) and exploitation (refining known optimal regions). Using the TA2 LWFA beamline we tested a custom Bayesian optimisation protocol as listed in Table 2. The optimisation loop was configured to vary a set of 6 Control Inputs: Dazzler settings, defocus, astigmatism 0 and 45, gas-cell length and gas pressure. This set of controls influence the following set of interdependent Physics

Inputs: laser pulse shape and duration, focal spot quality and position, gas density and profile. The objective function was chosen to maximise total electron charge at the accelerator output (Physics Output). Total electron charge was measured by integrating the total signal on the camera imaging the electron spectrometer lanex screen (Measured Outputs). Figure 7 demonstrates the optimisation run with an objective function of maximising total count on the electron spectrometer camera. The surrogate model was updated every 50 shots with a mean average – to mitigate the effect of a shot-to-shot jitter. The exploration phase dominated during the first 20 iterations, with a stable optimum found after 50 iterations. The inset in Fig. 7 shows a randomly chosen e-spec image during the first 100 and last 100 shots demonstrating 8-times gain in total electron charge.

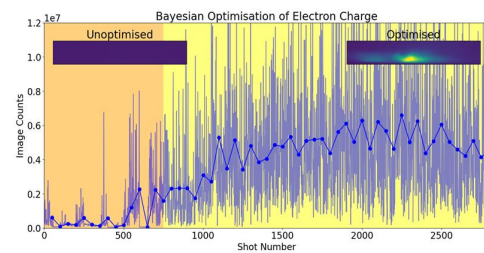


Figure 7: Total signal on the e-spec camera during optimisation process. Points show the mean average of each burst (50 shots) used to update the surrogate model.

Current work is focused on extending the optimisation to additional physics outputs, such as electron peak energy and beam divergence, with the goal of developing a robust, multi-objective optimisation framework for EPAC operations. In future, this approach can be naturally extended to reinforcement learning (RL) for continuous, adaptive control during long-duration runs, and to physics-informed machine learning strategies, where analytic models (e.g. beam transport) are combined with data-driven surrogates. These developments will enable faster convergence, better stability, and transferable models across facilities.

CONCLUSION

We have presented an overview of results from the development of a high-repetition-rate LWFA prototype for EPAC, including targetry durability studies, stability control and optimisation strategies. Our approach to the gas-cell design and choice of aperture material significantly increased the operation lifetime (by a factor of 10) and our Bayesian optimisation routine produced 8-times improvement in total electron charge with limited input controls. During EPAC commissioning in 2026, our work will expand towards stable multi-day operation of LWFA systems at the GeV-level for user-driven and industrial applications. A central focus will be the integration of machine-learning-based optimisation with advanced targetry and diagnostics to deliver reliable performance over extended runs.

REFERENCES

- [1] EPAC, Central Laser Facility,
<https://www.clf.stfc.ac.uk/Pages/EPAC-introduction-page.aspx>
- [2] A. R. Maier, N. M. Delbos, T. Eichner *et al.*, “Decoding Sources of Energy Variability in a Laser-Plasma Accelerator”, *Phys. Rev. X*, vol. 10, p. 031039, Aug. 2020.
[doi:10.1103/PhysRevX.10.031039](https://doi.org/10.1103/PhysRevX.10.031039)
- [3] I. Prencipe, J. Fuchs, S. Pascarelli *et al.*, “Targets for high repetition rate laser facilities: needs, challenges and perspectives”, *High Power Laser Sci. Eng.*, vol. 5, p. e17, 2017.
[doi:10.1017/hpl.2017.18](https://doi.org/10.1017/hpl.2017.18)
- [4] R. J. Shalloo, S. J. D. Dann, J. N. Gruse *et al.*, “Automation and control of laser wakefield accelerators using Bayesian optimization”, *Nat. Commun.*, vol. 11, p. 6355, Dec. 2020.
[doi:10.1038/s41467-020-20245-6](https://doi.org/10.1038/s41467-020-20245-6)
- [5] T. L. Audet, P. Lee, G. Maynard *et al.*, “Gas cell density characterization for laser wakefield acceleration”, *Nucl. Instrum. Methods Phys. Res. A*, vol. 12, pp. 383-386, Nov. 2018.
[doi:10.1016/j.nima.2018.01.053](https://doi.org/10.1016/j.nima.2018.01.053)
- [6] OpenFOAM CFD software, <https://openfoam.org>
- [7] K. Plamann and D. Fournier, “Thermal conductivity of CVD diamond: Methods and results”, *Phys. Status Solidi (a)*, vol. 154, no. 1, pp. 351-369, 1996.
[doi:10.1002/pssa.2211540125](https://doi.org/10.1002/pssa.2211540125)
- [8] Z. Q. Li, T. Sun, and J. Wang, “Atomistic simulations of ultrashort pulsed laser ablation of polycrystalline diamond,” *Curr. Nanosci.*, vol. 9, no. 6, pp. 727-732, Dec. 2013.
[doi:10.2174/1573413711309000098](https://doi.org/10.2174/1573413711309000098)